

GALAXIES IN FILAMENTS HAVE MORE SATELLITES: THE INFLUENCE OF THE COSMIC WEB ON THE SATELLITE LUMINOSITY FUNCTION IN THE SDSS

QUAN GUO

Leibniz-Institut für Astrophysik Potsdam, An der Sternwarte 16, D-14482 Potsdam, Germany

E. TEMPEL

Tartu Observatory, Observatooriumi 1, 61602 Tõravere, Estonia and
National Institute of Chemical Physics and Biophysics, Rāvala pst 10, Tallinn 10143, Estonia

N. I. LIBESKIND

Leibniz-Institut für Astrophysik Potsdam, An der Sternwarte 16, D-14482 Potsdam, Germany
Draft version September 14, 2018

ABSTRACT

We investigate whether the satellite luminosity function (LF) of primary galaxies identified in the Sloan Digital Sky Survey (SDSS) depends on whether the host galaxy is in a filament or not. Isolated primary galaxies are identified in the SDSS spectroscopic sample while potential satellites (that are up to 4 magnitudes fainter than their hosts) are searched for in the much deeper photometric sample. Filaments are constructed from the galaxy distribution by the “Bisous” process. Isolated primary galaxies are divided into two subsamples: those in filaments and those not in filaments. We examine the stacked mean satellite LF of both the filament and non-filament sample and find that, on average, the satellite LFs of galaxies in filaments is significantly higher than those of galaxies not in filaments. The filamentary environment can increase the abundance of the brightest satellites ($M_{\text{sat.}} < M_{\text{prim.}} + 2.0$), by a factor of ~ 2 compared with non-filament isolated galaxies. This result is independent of primary galaxy magnitude although the satellite LF of galaxies in the faintest magnitude bin, is too noisy to determine if such a dependence exists. Since our filaments are extracted from a spectroscopic flux-limited sample, we consider the possibility that the difference in satellite LF is due to a redshift, colour or environmental bias, finding these to be insufficient to explain our result. The dependence of the satellite LF on the cosmic web suggests that the filamentary environment may have a strong effect on the efficiency of galaxy formation.

Subject headings: large-scale structure of Universe — galaxies: luminosity function, mass function — galaxies: abundances.

1. INTRODUCTION

The Λ CDM model predicts that structure forms in a hierarchical manner. The first objects to collapse and virialize at high redshift are small dark matter haloes that later merge to form larger objects. Small haloes that host satellite or dwarf galaxies, can often survive the violent process associated with halo mergers for many Giga-years providing important information about galaxy formation, the population of subhaloes, and even the nature of dark matter.

Moreover these dark matter structures form an intricate pattern on the megaparsec scale, known as “cosmic web” (Bond et al. 1996), consisting of regions termed voids, filaments, sheets and knots. The cosmic web is a direct consequence of the gravitational instabilities that emerge out of the primordial density field. The presence of such cosmic pattern has been confirmed observationally by the distribution of the galaxies from the large surveys such as the 2dF Galaxy Redshift Survey (2dFGRS; Colless et al. 2001, 2003), the Sloan Digital Sky Survey (SDSS; York et al. 2000; Tegmark et al. 2004), the Two Micron All Sky Survey (2MASS; Huchra et al. 2005), Galaxy And Mass Assembly (GAMA; Alpaslan et al.

2014) and the CosmicFlow-2 survey of peculiar velocities (Tully et al. 2014).

A number of studies have examined how the cosmic web can affect specific halo properties such as abundance, shape, or assembly history (Aragón-Calvo et al. 2007; Hahn et al. 2007a,b; Libeskind et al. 2012, 2013a; Cautun et al. 2013). Correlations have also been found between halo spin and the principle axis of filaments (their spine) and walls (their normal) that they are embedded in (Altay et al. 2006; Aragón-Calvo et al. 2007; Hahn et al. 2007a,b; Zhang et al. 2009; Libeskind et al. 2013b; Aragon-Calvo & Yang 2014; Dubois et al. 2014). Although more difficult to quantify owing to degeneracies and inherent biases, similar studies have been conducted in observational samples (Jones et al. 2010; Tempel et al. 2013; Tempel & Libeskind 2013; Zhang et al. 2013). At $z = 3.1$ Matsuda et al. (2004) found that the spatial distribution of galaxies within $\text{Ly}\alpha$ haloes trace the underlying large-scale filamentary structure of the universe. The morphology and spatial extent of $\text{Ly}\alpha$ haloes depend on the environment as well (Matsuda et al. 2011, 2012).

Tying galaxy or halo properties to the environment is not a new idea and many studies have quantified the importance of such relations for galaxy formation and evolution (e.g. Dressler 1980; Kauffmann et al.

2004; Blanton et al. 2005; Tempel et al. 2011). On the larger scales of the cosmic web, the properties of galaxies depend on the cosmic filament it inhabits (e.g. Murphy et al. 2011; Jones et al. 2010) or on the supercluster environment (e.g. Lietzen et al. 2012; Einasto et al. 2014). However, to date no observational studies have examined the effect of the cosmic web environment on satellite galaxies.

Analyzing satellite systems of external galaxies is challenging, because typically only several satellites are detected per primary galaxy. Furthermore the real space position of a satellite with respect to its primary is uncertain. Owing to the advent of large galaxy surveys, a statistically robust estimate of the satellite luminosity function (LF) has become possible (e.g. Guo et al. 2011; Tal & van Dokkum 2011; Wang & White 2012).

In this study, we investigate if the satellite LF depends on whether the host galaxy is located within a filament. We divide isolated primary galaxies into two categories: those within galaxy filaments defined by the ‘‘Bisous process’’ as in Tempel et al. (2014) and those not in these filaments. Each subsample is then divided into three bins according to the primary’s magnitude. The resulting subsamples enable us to study the satellite LFs of isolated primary galaxies in filaments and compare it with isolated primary galaxies that are not in filaments. Such an analysis will quantify how the filament environment affects galaxy formation.

Throughout the paper we assume a fiducial Λ CDM cosmological model with $\Omega_M = 0.3$, $\Omega_\Lambda = 0.7$ and $H_0 = 70 \text{ km s}^{-1} \text{ Mpc}^{-1}$.

2. DATA AND METHODS

Throughout this paper we refer to isolated *primary* galaxies (or just ‘‘primaries’’) as the central galaxies that host systems of fainter satellites and fulfill a set isolation criteria, detailed below.

2.1. Galaxies and their satellites

The first step in our analysis is to identify isolated primaries. In order to do so we use the isolated primary catalogue selected by Guo et al. (2011, 2012).

Here, potential primaries are drawn from the SDSS DR8 spectroscopic survey. All galaxies within a projected distance of $2R_{\text{inner}}$ of a potential primary are examined (see below for the definition of R_{inner}). These must be more than half a magnitude fainter than a prospective host, unless the spectroscopic redshift difference is greater than 0.002. If a galaxy within $2R_{\text{inner}}$ only has a photometric redshift, then the host is considered isolated only if the difference between the host’s spectroscopic redshift and the interloper’s photometric redshift is greater than 2.5 times the photometric error. As a sanity check our isolated sample is cross matched with the group catalogue of Yang et al (2007) - an insignificant fraction of our primaries are considered members of groups according to Yang et al (2007). Omitting these has no discernible effect on our results. We use de-reddened *ugriz* bands model magnitudes and *k*-correct all galaxies to $z = 0$ with the IDL code of Blanton & Roweis (2007).

Satellite galaxies are drawn from both spectroscopic and photometric samples (Aihara et al. 2011). Since the photometric redshifts constrain the distance of a satellite

poorly, it is impossible to properly de-project a potential satellite. Thus a statistical background subtraction technique is used to estimate the real satellite galaxy population around each primary (see section 3 of Guo et al. (2011)). We begin by defining two radii, R_{inner} and R_{outer} . R_{inner} represents the projected radius within which satellites may reside. The annulus $R_{\text{outer}} - R_{\text{inner}}$ defines the region within which the local background is estimated. The luminosity function in this annulus is computed for each primary and then subtracted from the luminosity function within R_{inner} .

The values of R_{inner} and R_{outer} depend on the primary’s magnitude. We divide the primary sample into three *r*-band magnitude bins, each one magnitude wide and centred on $M_r = -21.0$, -22.0 , and -23.0 . The values of $(R_{\text{inner}}, R_{\text{outer}})$ are (0.3, 0.6), (0.4, 0.8) and (0.55, 0.9) Mpc, respectively (see Guo et al. (2012) for details on the choice of these values.) The magnitude bins correspond to haloes with mean virial radii of around 240, 370, 520 kpc respectively (Guo et al. 2012). Finally, the background-subtracted satellite LFs for each isolated primary in a given absolute magnitude bin is averaged, resulting in an estimate of the mean satellite LF. Guo et al. (2013) verified that the methodology described above returns the true satellite LF when applied to galaxy samples in simulations.

We also examine the projected number density profiles of satellites more luminous than a particular absolute magnitude (in Appendix B, as described more fully in Guo et al. 2011, 2012). Such density profiles are shown in units of r_{200} and divided by the total number of satellites within this radius. The values of r_{200} are the same as in Guo et al. (2012, 2013) and equal to 0.24, 0.37, 0.52 Mpc for three magnitude bins respectively.

Finally, the effects of incompleteness and other biases are examined in Appendix A.

2.2. SDSS galaxy filaments

The catalogue of filaments is built by applying an object point process with interactions (the Bisous process) to the distribution of galaxies in the spectroscopic galaxy sample from SDSS DR8 as described in Tempel et al. (2014). Random small segments (cylinders) based on the positions of galaxies are used to construct a filamentary network by examining the connectivity and alignment of these segments. A filamentary spine can then be extracted based on a detection probability and filament orientation (see Tempel et al. 2014).

The catalogue of filaments (‘‘filament spines’’) we use in this study is the same that of Tempel et al. (2014), where the assumed filament radius is roughly 0.71 Mpc. This means that primary galaxies in filaments are less than 0.71 Mpc from the filament spine. This catalogue is constructed from the full spectroscopic galaxy sample with lower and upper CMB-corrected distance limits of $z = 0.009$ and $z = 0.155$ respectively. We thus confine our analysis to this redshift range. Filaments at higher redshift than the upper limit are too ‘‘diluted’’ to be detected. We classify a galaxy as ‘‘in-a-filaments’’ if the distance of the galaxy from the axis of the filament is less than 0.71 Mpc and the distance of the galaxy from the end point of filament (if the galaxy is outside a filamentary cylinder) is less than 0.14 Mpc.

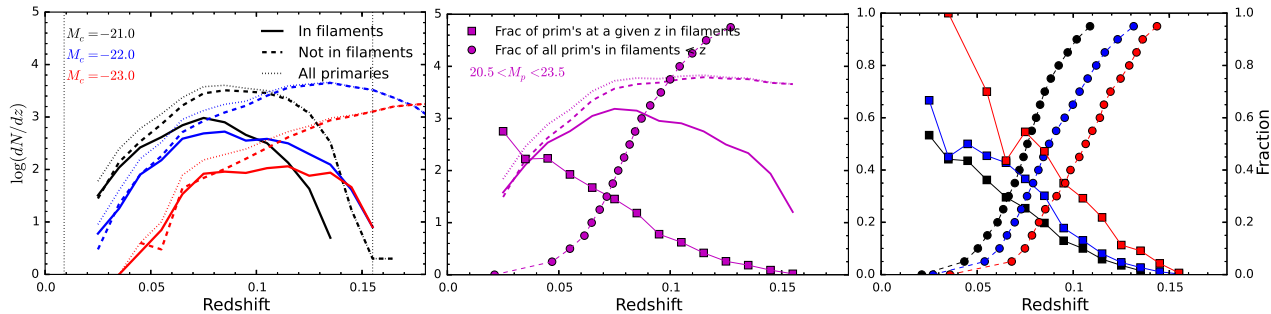


Figure 1. *Left:* The redshift distribution of our primary sample, divided into three magnitude bins centered on $M_r = -21.0$, -22.0 , -23.0 (shown in black, blue, and red respectively). The dotted, dashed and solid lines show these distributions for all primaries, those found in filaments and those not in filaments (respectively). The two vertical thin dotted lines indicate the upper and lower z limit of the filament catalogue. *Center:* the redshift distribution for all primaries at all magnitudes (i.e. $-20.5 < M_r < -23.5$) is line coded by filamentary environment according to the same scheme. The lines connected by squares and circles indicate the fraction of primaries at given redshift found in filaments and the and the fraction of all primaries that are in filaments below a given z . *Right:* the same two fractions shown divided by magnitude.

2.3. Redshift biases

For each magnitude bin $M_r = -21, -22, -23$ there are 4425 (22795), 3077 (27857), 740 (4875) primaries in filaments (not in filaments). Thus the fraction of isolated galaxies in filaments is roughly 18.5%, 11.0% and 15.1%, respectively. The (normalized) redshift distribution of primaries (in and not in filaments) is shown in the left panel of Figure 1. At a given magnitude, the redshift distribution of galaxies in filaments tends to peak at lower z than those not in filaments. In the right panel of Figure 1 we show the fraction of isolated galaxies in filaments as a function of redshift for our three magnitude bins. These vary from $\sim 50\%$ at low z to $\sim 0\%$ at the limit of our redshift range.

Such a dramatic drop is mainly driven by the filament finding algorithm: the probability of detecting filaments decreases significantly in the redshift range considered here (namely from $z = 0.009$ to 0.15 , see Tempel et al. 2014). This is because filaments are identified in the flux-limited galaxy sample: as one goes to higher z the number density of galaxies decreases significantly, making the identification of filaments more difficult. Also note that the catalogue from which primaries are drawn is also flux-limited: the number of galaxies also decreases with redshift. Thus the combined effect of lower number density of isolated galaxies with fewer identifiable filaments at high redshift results in the number of isolated galaxies in filaments going to null at $z > 0.15$. Therefore the dramatic drop of primaries found in filaments at higher z is *not* a real feature of the galaxy distribution.

Therefore, we exclude galaxies at high ($z > 0.15$) and at low ($z < 0.04$) redshifts, since these redshifts are not well covered by the filament catalogue. We only consider primaries in the redshift ranges $0.04 < z < 0.13$, $0.04 < z < 0.14$ and $0.06 < z < 0.15$ for magnitudes of -21 , -22 and -23 respectively, in order to ensure that the fraction of primaries in filaments is kept at around ($\sim 50\%$).

3. RESULTS

The satellite LF for primaries in and not in filaments is shown in top panel of Figure 2. For the magnitude bin $M_c^r = -21.0$, the small number of primaries results in a LF that is too noisy to show any difference (if one existed): the mean number of satellites around these low luminosity primary galaxies is intrinsically lower than

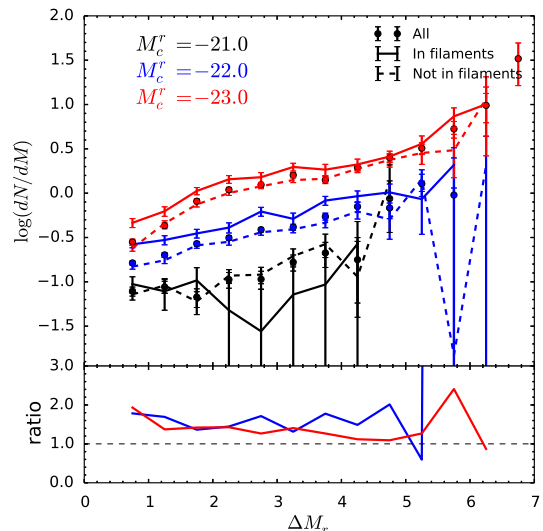


Figure 2. The satellite LF (top panel) for all primary galaxies, those in filaments and those not in filaments is shown as points, solid lines and dashed lines, respectively for three different magnitude bins $M_r = -21.0$, -22.0 , -23.0 (black, blue and red lines, respectively). The ratio of the satellite LFs of galaxies in filaments to those in the same magnitude bin but not in filaments is shown in bottom panel (for $M_r = -22.0, -23.0$).

that of brighter primaries and the number of these low-luminosity primaries found in filaments is not sufficiently high to have good signal-to-noise ratio.

Beyond the faintest magnitude bin, the satellites LF of primaries in filaments (extending to at least 4 magnitudes fainter than the primary) is significantly higher than those of primaries that are not in filaments. At the bright end of the satellite LFs we find that there are roughly double the number of satellites around primaries that are in filaments compared those that are not in the filaments. This is our main result: *at a given magnitude, isolated galaxies in filaments have more bright satellites than isolated galaxies that are not in filaments.*

Since the fractions of galaxies in filaments varies significantly with the redshift, we wish to test whether the difference in the satellite LFs we have seen is caused by the bias in the redshift distribution. We thus perform a number of tests described in Section 3.1 to 3.3.

3.1. Applying weights to the Satellite LFs

Suppose our main result - that galaxies in filaments have *on average* more satellites - is driven by the a redshift evolution of the satellite LF combined with the decreasing likelihood in finding isolated primaries in filaments. In order to control for this possibility, the contribution to the mean “not-in-filament” satellite LF from a given primary is weighted according to what fraction of all galaxies, at that z , are found in filaments and what fraction are not. For example, at $0.07 < z < 0.08$ most galaxies (68%) (in magnitude bin $M_c^r = -22.0$) are not in filaments. Thus when we compute the contribution for a primary that is not found in filaments and in this redshift range to the mean LF, we weigh its satellite LF by 0.47 ($=32/68$). In this way redshift ranges where filaments are easily detected and redshift ranges where filaments are not easily detected are given inverse weights. If the result we have found is driven by a redshift dependent satellite LF, such a test should give identical satellite LFs for in filament and not-in-filament samples. The satellite LF with weighting is thus estimated as:

$$\overline{N}_j = \frac{\sum_{i=1}^{N_j} W_i N_i(M_j)}{\sum_{i=1}^{N_j} W_i}, \quad (1)$$

where N_i is the number of satellites around primary galaxy i , W_i is the weight for the primary galaxy i and N_j is the number of primaries contributing to the j th bin of the LF. The weight W_i for each primary galaxy is determined by the aforementioned way.

The top panels of Figure 3 shows the resulting satellite LFs with the aforementioned weighting from the redshift distribution of primary galaxies not in filaments for the magnitude bins $M_c^r = -22.0$ and -23.0 . The weighted satellites LF for in filament primaries is still significantly different from those not in filaments (in a given magnitude bin). Note that the weighted satellite LFs for primaries not in filaments are noisier because fewer primaries are able to contribute to the estimation of the mean satellite LFs. This suggests that the redshift bias cannot account for the differences between the satellite LFs in filaments.

Now, suppose our main result is driven by the primary colour distribution. A similarly weighted satellite LFs can be estimated in the same way but with weightings determined such that the distribution of $(g-r)$ colours (rather than the distribution of redshifts) between filament and non-filament primaries match. Again, such a LF suggests that a potential colour bias also fails to account for the difference in satellite LF (see the bottom panel of Figure 3).

Another source of possible systematic bias is the different environmental densities around primary galaxies in filaments and not in filaments. This has been checked and statistically the primary galaxies in filaments and not in filaments have the same distribution of environmental densities. In summary: *the difference in filament and non-filament satellite LF cannot be attributed to an underlying colour, redshift or environmental density bias. The filament and non-filament satellite LFs are intrinsically different.*

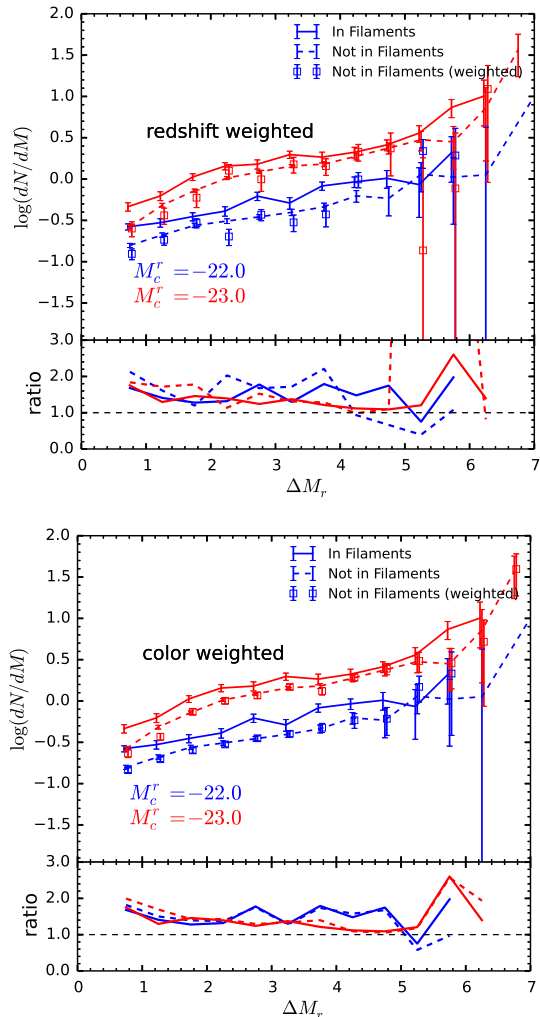


Figure 3. Tests of whether the difference in the mean satellite LF is due to the different redshift (top) or color (bottom) distributions of filament/not-in-filament primaries, are shown here. Accordingly, the contribution to the mean satellite LF due to a not-in-filament primary is weighted by the fraction of all primaries (at that z , top or with that color, bottom) that are found in filaments. The weighted not-in-filament satellite LF is shown by squares while the not-in-filament one is shown by the dashed lines. The unweighted satellite LF for filament primaries is shown for reference (solid lines). The small bottom panels show the ratio of the satellite LFs of in-filaments galaxies to those of not-in-filaments galaxies as well as the ratio of satellite LFs of in-filaments galaxies to the weighted satellite LFs of not-in-filaments galaxies as dashed lines. Color coding is the same as in Fig. 2.

3.2. Dependence on the redshift of primary galaxies

To further explore how the changing fractions of primaries in-filaments can influence the differences between the satellite LFs, we split the in-filaments and not-in-filaments primaries into “near” ($0.04 < z < 0.09$, $0.05 < z < 0.11$ for $M_c^r = -22.0, -23.0$ respectively) and “far” ($0.09 < z < 0.14$, $0.11 < z < 0.15$) subsamples. The resulting satellite LFs for these subsamples are shown in Fig. 4. The satellites LFs for in filament and not-in-filament primaries are still significantly different for both near and far subsamples, although the differences in far subsamples are smaller than those in near subsamples. This could be caused by the fact that the contamination in not-in-filaments primaries in far subsamples

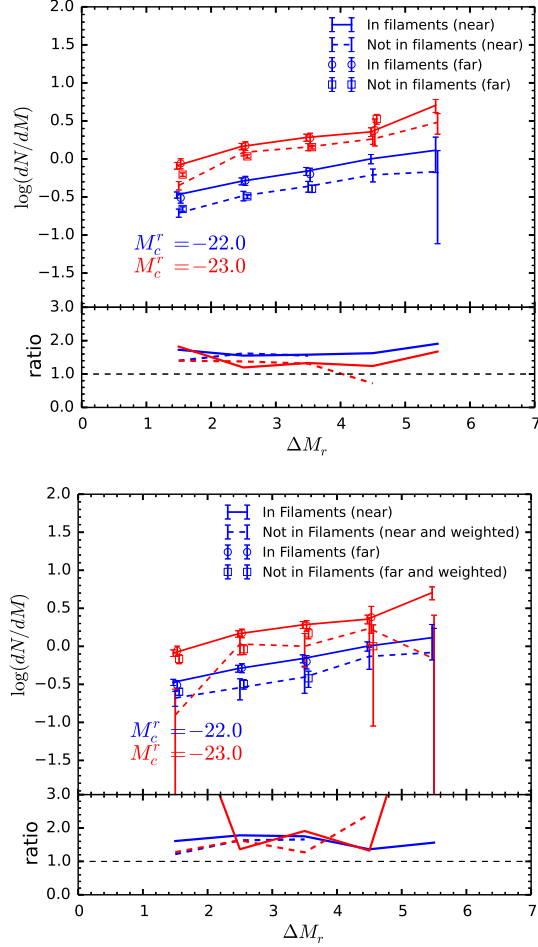


Figure 4. Similar to Figure 3, but where the weighting is done with respect to “near” and “far” subsamples. *Top:* We show the mean satellite LF for in-filaments galaxies in the near subsample (solid lines), in-filaments primaries in the far subsample (open circles), not-in-filaments primaries in near subsample (dashed lines) and not-in-filaments primaries in far subsample (open squares). The ratio of the two near (far) subsamples are shown in the lower panel as the solid (dashed) lines. *Bottom:* the satellite LF of the not-in-filament primaries is weighted as in Figure 3. The codes of colours are the same as in Fig. 2.

is higher than that in near subsamples, i.e. more in-filaments galaxies in far subsamples may be mis-classified as not-in-filaments. The weighted satellite LFs of galaxies not in filaments are shown in the two bottom panels of Fig. 4 as an attempt to minimise the redshift-bias between the in-filament galaxies and the not-in-filaments ones in both near and far subsamples. Due to the small number of primaries in the subsamples which are able to contribute the estimation of the weighted satellite LFs, the results are quite noisy. However the difference between the mean of satellite LFs in filaments and not in filaments can still be seen.

In each magnitude bin, only around 15% of isolated galaxies are found in filaments. We wish to check if the difference in the satellite LF is due to the variance of this small fraction. We do so by comparing the mean in-filament satellite LFs to the mean of (a random set of) 500 not-in-filament satellite LFs. This set of 500 random satellite LFs matches both the redshift range and the number of the in-filaments galaxies. Again, we

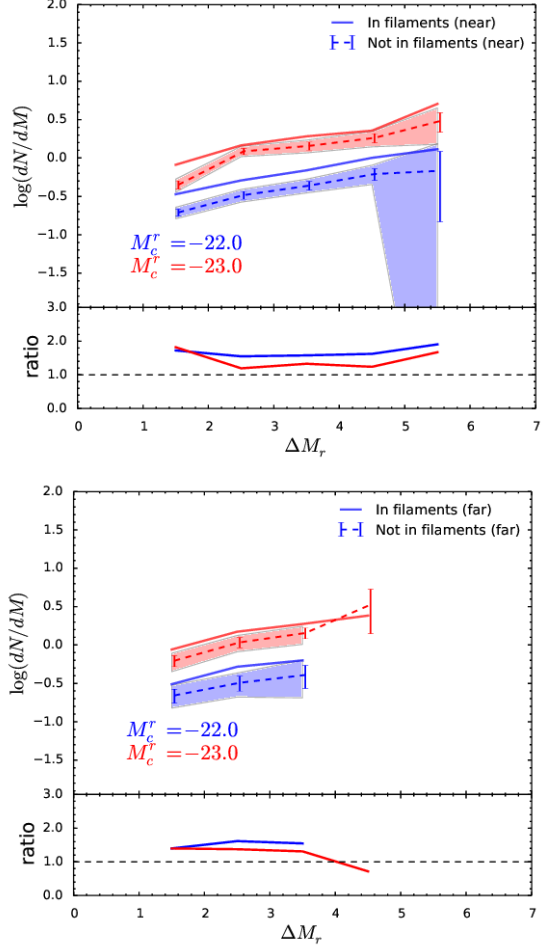


Figure 5. The mean satellite LFs composed by randomly selecting 500 primaries from filament primaries (solid line) and not-in-filament primaries (dashed) in near (top) and far (bottom) samples. The error bars show the 1σ standard deviation of the distribution of the mean satellite LFs. The shaded regions show the corresponding 5^{th} and 95^{th} quantiles. The small lower panels show the ratios of corresponding mean satellite LFs as in previous Figures. Curves are color coded by magnitude as in previous figures

split these into near and far samples. Figure 5 shows the results of comparing these. The difference between the mean satellite LFs of in-filaments galaxies and of a randomly drawn, equally sized and redshift distributed not-in-filaments sample in both near and far ranges, is robust and statistically significant (at the $\sim 2\sigma$ level).

Is our result valid if the redshift range is confined to small interval? In Figure 6 we show the satellite LF in two relatively narrow redshift slices ($0.07 < z < 0.09$, $0.08 < z < 0.10$ for $M_c^r = -22.0, -23.0$). In these narrow redshift ranges, the fractions of in-filaments primaries varies very little. The comparison of satellite LFs is thus less biased by counting statistics. Moreover, bright satellites in these redshift slices are quite far from the faint limits of the SDSS. The estimation of the mean satellite LFs is therefore less affected by possible incompleteness. The results from these subsamples again show that the mean satellite LFs of in-filaments galaxies and not-in-filaments galaxies are significantly different.

To summarize: the difference between the satellite LFs of in-filament and not-in-filament primaries are seen in a wide range of subsamples. The fact that the fraction of

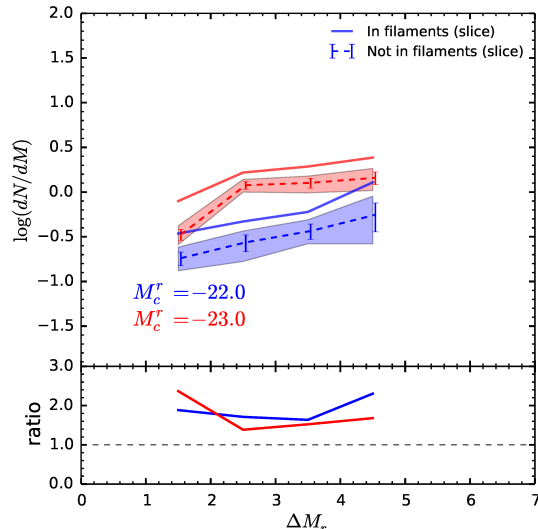


Figure 6. Same as Figure 5, but for a narrow redshift slices ($0.07 < z < 0.09$, $0.08 < z < 0.10$ for $M_r = -22.0, -23.0$ respectively).

galaxies in-filaments varies with the redshift dramatically is thus insufficient to explain the difference in the satellite LF.

3.3. Control sample

Besides the different redshift and colour distributions of the two samples, the classification of primaries as in-filaments and not-in-filaments could introduce other potential biases which can individually or together result in the differences seen here. To take such an effect into account, we build control samples from the not-in-filament catalogue. We then compare the mean satellite LFs estimated from galaxies in-filaments with a corresponding control samples of galaxies not-in-filaments. For each primary found in a filament, we select a unique counterpart from the corresponding not-in-filament control sample. The counterpart is selected to have the same $g - r$ colour, visible axis ratio b/a , redshift and magnitude. Given a filament primary, we select a counterpart by finding the not-in-filament galaxy which minimizes the following cost :

$$C = \sqrt{\left(\frac{\Delta z}{0.036}\right)^2 + \left(\frac{\Delta M_r}{0.75}\right)^2 + \left(\frac{\Delta(g-r)}{0.15}\right)^2 + \left(\frac{\Delta(b/a)}{0.25}\right)^2}, \quad (2)$$

where the quantities Δz , ΔM_r , $\Delta(g - r)$, and $\Delta(b/a)$ are the difference between the redshift, r band magnitude, $g - r$ colour and axis ratio between the filament primary and not-in-filament candidate. The denominators of each term are the scaling factors that correspond to the standard deviation of distribution of each quantity.

The general properties of our control sample drawn from primaries not-in-filaments is shown in Figure 7. Note that our technique of minimizing the cost C is successful: Figure 7 shows little difference between in filament primaries and the control sample. This makes the comparison of the mean satellite LFs from these two groups less biased. Figure 8 shows the mean satellite LFs of in-filaments and not-in-filaments galaxies of

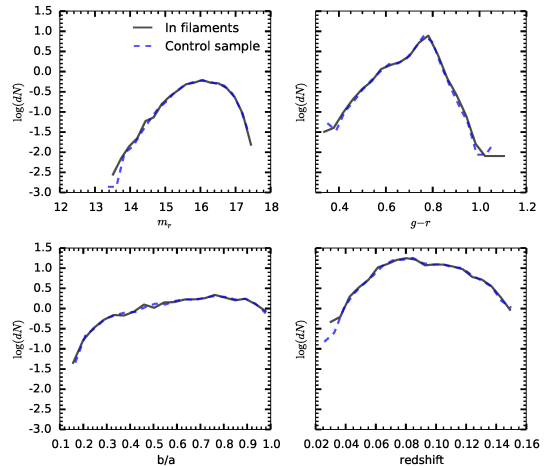


Figure 7. A comparison of the properties of filament primaries (solid lines) with their not-in-filaments twins that constitute our control sample (dashed lines) for magnitude bin $M_c^r = -22.0$.

the control samples, which again confirms the differences between the satellite LFs of in-filaments and not-in-filaments galaxies is not caused by a possible bias in the distribution of magnitudes, redshift, colour, or visible axis ratio of the primary galaxies.

4. SUMMARY AND CONCLUSIONS

We have examined the luminosity function (LF) of satellites close to isolated primary galaxies in the SDSS. Isolated primary galaxies have been split by filamentary environment into two camps: those primaries in and not in filaments. Background galaxies are subtracted statistically and the mean satellite LF is computed by stacking all centrals of a given absolute r band magnitude.

Our results indicate that primaries in filaments have more satellites than those that are not found in filamentary environments. This is most evident for the brightest satellites but is true for satellites up to 4 magnitudes fainter of their host. Except for the faintest magnitude bin (where the signal-to-noise is too low to judge), in-filament primaries have a factor of ~ 1.5 – 2 more bright satellites than primaries not in filaments. This slightly varies with redshift possibly because the contamination in the sample of galaxies not in filaments increases with the redshift.

We have examined if the difference in the satellite LF is due to other controlling factors including differences in colour, density, redshift distribution or variance of small sample sizes. None of these control factors can explain the result found here. The differences exhibited are statistically significant and robust and thus reflect an inherent difference in the satellite population of galaxies in and not in filaments.

We have also examined the mean radial distribution of satellites brighter than a r -band magnitude of -20 in Appendix B and found no significant difference in the projected spatial distribution of satellites in or not in filaments in spite of the obvious difference between the total numbers of satellites.

Previous numerical studies have shown that the abundance of dark matter subhaloes may depend on the environment: haloes in filaments may have more subhaloes than those in other cosmic web environments (Cautun et

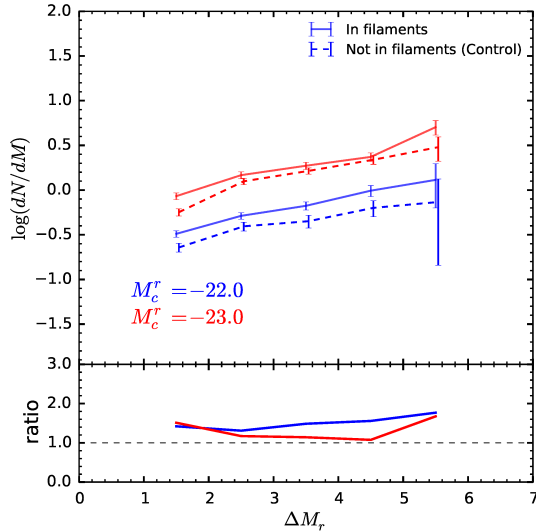


Figure 8. The mean satellite LFs of in-filaments primaries (solid lines) and a control sample of “twins” chosen from the not-in-filaments sample (dashed lines) according to Equation 2, color coded by magnitude. The ratio of the satellite LFs of in-filaments and not-in-filaments are shown in the small lower panel.

al. in preparation; Neyrinck et al. 2014). The properties of subhaloes in filaments can be also different from those in the other environments and this may affect galaxy formation since the satellite LF is a result of the gas physics that regulate star formation in small haloes. Our results thus suggest that galaxy formation itself may be more efficient in subhaloes that are born in and accreted through filaments. The filamentary environment may be a crucial component of galaxy formation on such small scales.

ET acknowledge the ESF grants MJD272, IUT40-2 and the European Regional Development Fund. NIL acknowledges a grant from the *Deutsche Forschungs Gemeinschaft*. Funding for SDSS-III has been provided by the Alfred P. Sloan Foundation, the Participating Institutions, the National Science Foundation, and the U.S. Department of Energy Office of Science. The SDSS-III web site is <http://www.sdss3.org/>. SDSS-III is managed by the Astrophysical Research Consortium for the Participating Institutions of the SDSS-III Collaboration including the University of Arizona, the Brazilian Participation Group, Brookhaven National Laboratory, Carnegie Mellon University, University of Florida, the French Participation Group, the German Participation Group, Harvard University, the Instituto de Astrofísica de Canarias, the Michigan State/Notre Dame/JINA Participation Group, Johns Hopkins University, Lawrence Berkeley National Laboratory, Max Planck Institute for Astrophysics, Max Planck Institute for Extraterrestrial Physics, New Mexico State University, New York University, Ohio State University, Pennsylvania State University, University of Portsmouth, Princeton University, the Spanish Participation Group, University of Tokyo, University of Utah, Vanderbilt University, University of Virginia, University of Washington, and Yale University.

REFERENCES

- Aihara, H., Allende Prieto, C., An, D., et al. 2011, *ApJS*, 193, 29
- Alpaslan, M., Robotham, A. S. G., Driver, S., et al. 2014, *MNRAS*, 438, 177
- Altay, G., Colberg, J. M., & Croft, R. A. C. 2006, *MNRAS*, 370, 1422
- Aragon-Calvo, M. A., & Yang, L. F. 2014, *MNRAS*, 440, L46
- Aragón-Calvo, M. A., van de Weygaert, R., Jones, B. J. T., & van der Hulst, J. M. 2007, *ApJ*, 655, L5
- Blanton, M. R., Eisenstein, D., Hogg, D. W., Schlegel, D. J., & Brinkmann, J. 2005, *ApJ*, 629, 143
- Blanton, M. R., & Roweis, S. 2007, *AJ*, 133, 734
- Bond, J. R., Kofman, L., & Pogosyan, D. 1996, *Nature*, 380, 603
- Cautun, M., van de Weygaert, R., & Jones, B. J. T. 2013, *MNRAS*, 429, 1286
- Colless, M., Dalton, G., Maddox, S., et al. 2001, *MNRAS*, 328, 1039
- Colless, M., Peterson, B. A., Jackson, C., et al. 2003, *ArXiv Astrophysics e-prints*, astro-ph/0306581
- Dressler, A. 1980, *ApJ*, 236, 351
- Dubois, Y., Pichon, C., Welker, C., et al. 2014, *ArXiv e-prints*, arXiv:1402.1165
- Einasto, M., Lietzen, H., Tempel, E., et al. 2014, *A&A*, 562, A87
- Guo, Q., Cole, S., Eke, V., & Frenk, C. 2011, *MNRAS*, 417, 370
- , 2012, *MNRAS*, 427, 428
- Guo, Q., Cole, S., Eke, V., Frenk, C., & Helly, J. 2013, *MNRAS*, 434, 1838
- Hahn, O., Carollo, C. M., Porciani, C., & Dekel, A. 2007a, *MNRAS*, 381, 41
- Hahn, O., Porciani, C., Carollo, C. M., & Dekel, A. 2007b, *MNRAS*, 375, 489
- Huchra, J., Jarrett, T., Skrutskie, M., et al. 2005, in *Astronomical Society of the Pacific Conference Series*, Vol. 329, *Nearby Large-Scale Structures and the Zone of Avoidance*, ed. A. P. Fairall & P. A. Woudt, 135
- Jones, B. J. T., van de Weygaert, R., & Aragón-Calvo, M. A. 2010, *MNRAS*, 408, 897
- Kauffmann, G., White, S. D. M., Heckman, T. M., et al. 2004, *MNRAS*, 353, 713
- Libeskind, N. I., Hoffman, Y., Forero-Romero, J., et al. 2013a, *MNRAS*, 428, 2489
- Libeskind, N. I., Hoffman, Y., Knebe, A., et al. 2012, *MNRAS*, 421, L137
- Libeskind, N. I., Hoffman, Y., Steinmetz, M., et al. 2013b, *ApJ*, 766, L15
- Lietzen, H., Tempel, E., Heinämäki, P., et al. 2012, *A&A*, 545, A104
- Matsuda Y. et al., 2004, *AJ*, 128, 569
- Matsuda Y. et al., 2011, *MNRAS*, 410, L13
- Matsuda Y. et al., 2012, *MNRAS*, 425, 878
- Murphy, D. N. A., Eke, V. R., & Frenk, C. S. 2011, *MNRAS*, 413, 2288
- Neyrinck M. C., Aragón-Calvo M. A., Jeong D., Wang X., 2014, *MNRAS*, 441, 646
- Tal, T., & van Dokkum, P. G. 2011, *ApJ*, 731, 89
- Tegmark, M., Blanton, M. R., Strauss, M. A., et al. 2004, *ApJ*, 606, 702
- Tempel, E., & Libeskind, N. I. 2013, *ApJ*, 775, L42
- Tempel, E., Saar, E., Liivamägi, L. J., et al. 2011, *A&A*, 529, A53
- Tempel, E., Stoica, R. S., Martínez, V. J., et al. 2014, *MNRAS*, 438, 3465
- Tempel, E., Stoica, R. S., & Saar, E. 2013, *MNRAS*, 428, 1827
- Tully, R. B., Courtois, H., Hoffman, Y., & Pomarède, D. 2014, *Nature*, 513, 71
- Wang, W., & White, S. D. M. 2012, *MNRAS*, 424, 2574
- York, D. G., Adelman, J., Anderson, Jr., J. E., et al. 2000, *AJ*, 120, 1579
- Zhang, Y., Yang, X., Faltenbacher, A., et al. 2009, *ApJ*, 706, 747
- Zhang, Y., Yang, X., Wang, H., et al. 2013, *ApJ*, 779, 160

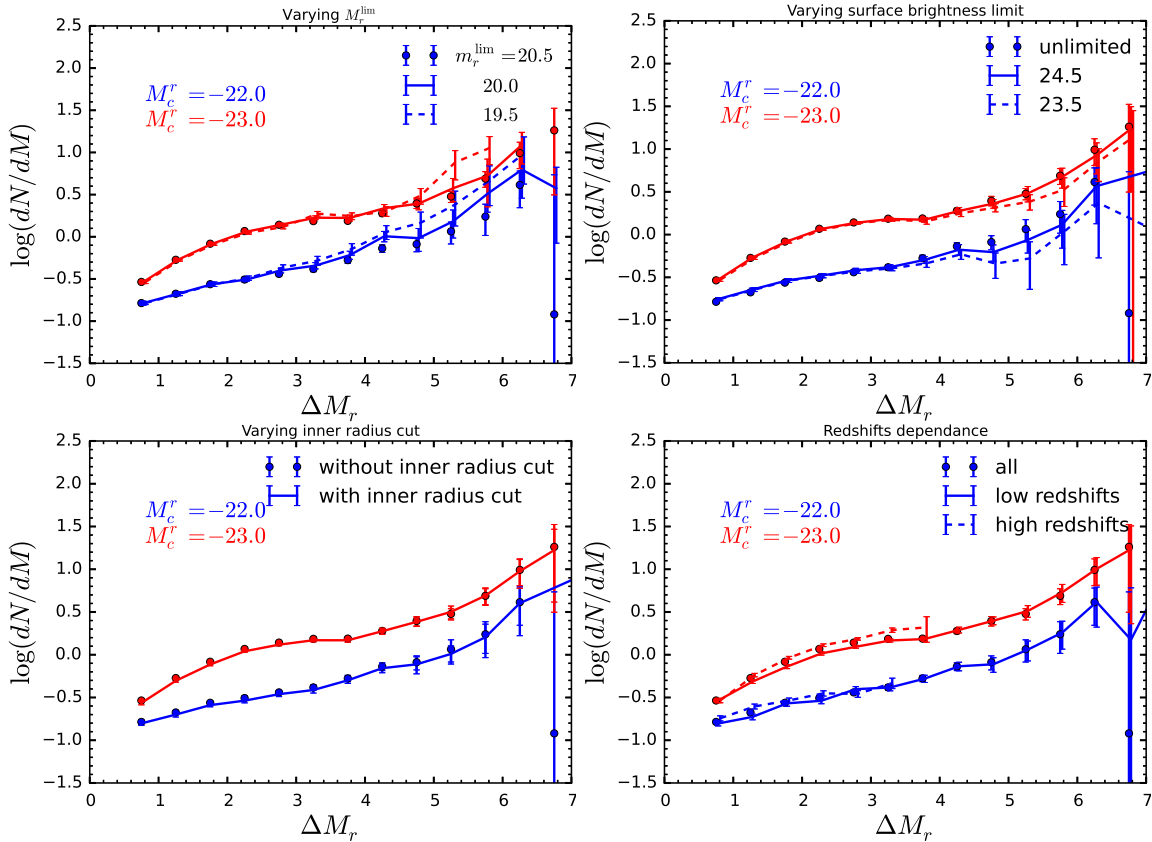


Figure 9. The effect on the satellite LFs of varying the magnitude limit, m_r^{lim} (upper left), the surface brightness limit (upper right), the inner radius (bottom left), and splitting the primary galaxies in the subsamples at low and high redshift (bottom right). The satellite LF with different parameters and default parameter are shown as solid, dashed lines and filled points respectively. The color coding is same as in previous figures.

APPENDIX

TEST OF THE ESTIMATION OF SATELLITE LFS

In Figure 5 of Guo et al. (2011), the estimated satellite LFs were tested and found to be robust to changes in the values of selection parameters: ΔM_{bin} , ΔM_{faint} , Δz_s , α_p , m_v^{lim} . Here we perform a few more tests to see if our estimated satellite LFs are also robust in terms of other possible incompleteness or biases. In the upper right panel of Fig. 9 (titled: “varying the magnitude limit m_r^{lim} ”), we reduce the faint magnitude cut of the input catalogue used for searching for satellites. The resulting satellite LFs at the bright end is nearly identical. Such a cut causes only small variations in the faint end of the satellite LFs. A similar situation is seen if we vary the surface brightness cut for the input catalogue (upper right of Fig. 9). Figure 5 of Guo et al. (2011) shows that the galaxy catalogue is not complete due to preferentially missing low surface brightness galaxies. With the bright magnitude cut, such incompleteness is greatly reduced. Therefore varying the surface brightness cut does not affect the satellite LFs. In the region close to the primary galaxies, spiral arms fragments could be occasionally erroneously misclassified as separate galaxies. Moreover the completeness in the region close to primary is poor since the light of the central galaxy dominates this region. For such incompleteness, we compare the satellite LFs estimated with and without excluding the galaxies within a radius of 1.5 times the Petrosian R_{90} of the primary galaxies, shown in the lower left panel in Fig. 9 (entitled “varying the inner radius cut”). The result shows that such incompleteness is not important in the computation of the satellite LF. This is because the R_{90} is small. We thus infer that objects found at these distances contribute little to the mean satellite LFs. In the bottom right panel of Fig. 9, we test the dependence of the estimated satellite LFs on the redshift of primary galaxies. The primary galaxies are split into subsamples at low and high redshift according to the median of the redshift distribution of all isolated galaxies in the magnitude bins. The satellites LFs estimated from the sample of primary galaxies at low redshift are compared with those from the sample of primary galaxies at high redshift, shows that only for the $M_c^r = -23.0$ bin is the satellite LFs slightly different. However, such variation is not enough to account for the difference between the satellite LFs of in-filaments galaxies and not-in-filaments galaxies. For tests of the dependence on the redshift of primary galaxies we refer the reader to the Section 3.2 for more details.

In summary, our tests show that our estimated satellite LFs of isolated primaries, especially the bright end, are quite robust to parameter selections, incompleteness or biases. There is thus no evidence that the differences in the satellite LFs of in-filaments and not-in-filament galaxies is anything other than a real physical effect.

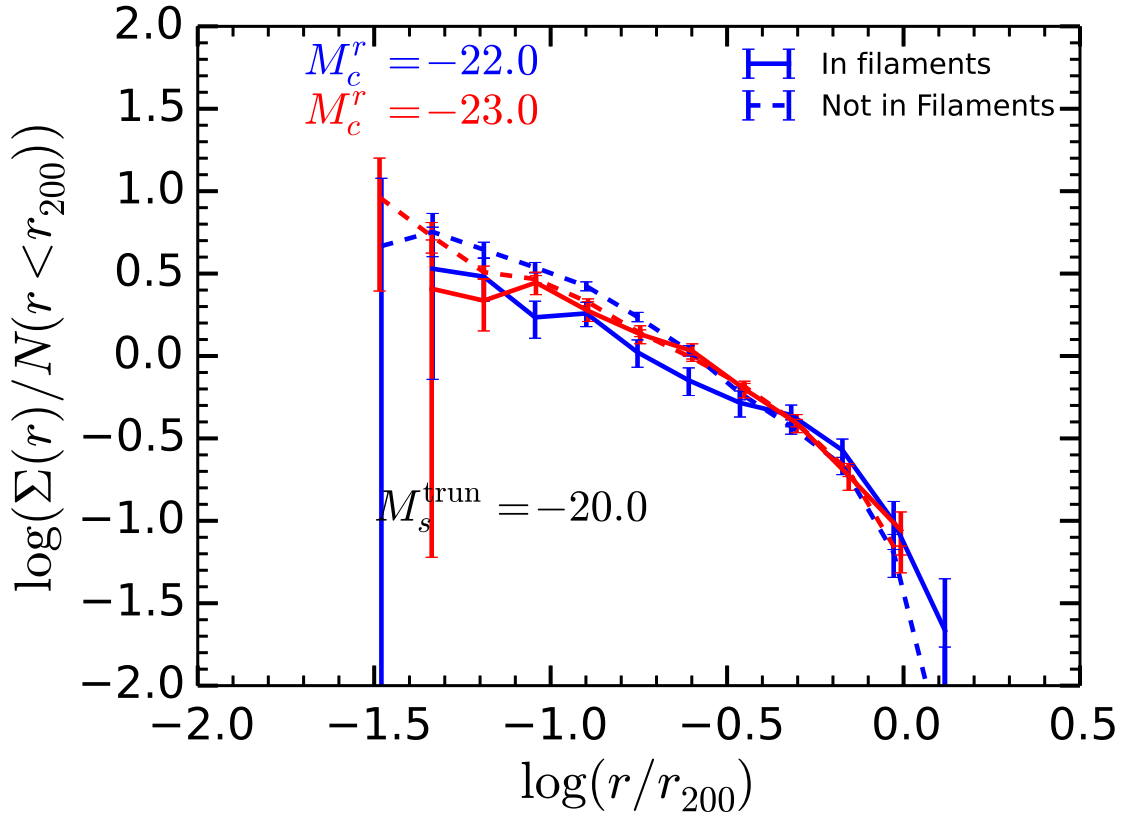


Figure 10. The scaled projected density profiles of satellites brighter than -20 magnitude in r band for the primary galaxies in filaments and not in filaments. The codes of legends are the same as in Fig. 2.

PROJECTED RADIAL DISTRIBUTION

The difference at the bright end of the satellite LFs for these two subsamples is most significant in the brightest two magnitude bins. We therefore show the radial distribution of satellites in and not in filaments (for $M_c^r = -22.0, -23.0$) in Figure 10. In spite of the fact that the total number of satellites depends strongly on whether the primary is inside a filament or not, the mean radial distributions of satellites in these two environments are remarkably similar to each other. However for the magnitude bin $M_c^r = -22.0$, the radial distribution of satellites brighter than -20 magnitude in r band seems slightly less centrally concentrated in filaments than not-in-filaments. This may be caused by the limited volume of the primary galaxies in filaments, since the result is relative noisy.